# Bistable Latch Ising Machines

Jaijeet Roychowdhury(✉)

Department of Electrical Engineering and Computer Sciences,
University of California, Berkeley, CA 94720, USA
jr@berkeley.edu

**Abstract.** Ising machines have been attracting attention due to their ability to use mixed discrete/continuous mechanisms to solve difficult combinatorial optimization problems. We present BLIM, a novel Ising machine scheme that uses latches (bistable elements) with controllable gains as Ising spins. We show that networks of coupled latches have a Lyapunov or "energy" function that matches the Ising Hamiltonian in discrete operation, enabling them to function as Ising machines. This result is established in a general coupled-element Ising machine framework that is not limited to BLIM. Operating the latches periodically in analog/continuous mode, during which bistability is removed, helps the system traverse to better minima. CMOS realizations of BLIM have desirable practical features; implementation in other physical domains is an intriguing possibility.

## 1 Introduction

Over the last decade, hardware Ising machines have emerged as a promising means to solve classically difficult (*e.g.*, NP-complete) computational problems. The premise of Ising machines is that specialized hardware implementing the Ising computational model (see Sect. 2) can solve difficult combinatorial problems more effectively than classical algorithms (such as semidefinite programming and simulated annealing [7,10]) run on digital computers. Ising machines first came into prominence with the D-Wave quantum annealer [2,8] and the Coherent Ising Machine (CIM) [14,18,19]. A D-Wave quantum annealer with 5000 spins is available commercially; CIM with 2000 spins has been successfully demonstrated at NTT Research Labs, with larger systems under active development. Although they have established the field of Ising machines and inspired follow-on technologies, D-Wave's quantum annealer and CIM are physically large, expensive, and difficult to miniaturize or scale to larger problems. A few years ago, we showed that networks of coupled oscillators can be designed to function as Ising machines [3,15–17]. Such oscillator Ising machines (OIMs) changed the technology landscape for Ising machines by bringing them within the realm of miniaturizable CMOS electronics, with all the size, cost, speed, energy efficiency, scalability and mass production benefits that accrue as a result.

We now present the Bistable Latch Ising Machine (BLIM), a new way to build Ising machines that employs simple bistable elements, *i.e.*, latches, a familiar


I. Kostitsyna and P. Orponen (Eds.): UCNC 2021, LNCS 12984, pp. 131–148, 2021.
https://doi.org/10.1007/978-3-030-87993-8_9

and ubiquitous element in electronics.[1] BLIM is enabled by a result (Sect. 3) that establishes that networks of coupled latches have an "energy[2] function" that is naturally minimized, leading to good solutions of the Ising problem. That latches can be used as substrates represents a broadening, both theoretical and practical, of the Ising machine landscape, while enhancing the advantages of miniaturizability/scalability, low cost, and mass production introduced by OIM. Latches are simpler elements than oscillators, with basic versions requiring only 4 CMOS transistors. Importantly, the formulation in which we prove our main result is a general one, not limited to latches—it encompasses OIM and, potentially, other types of Ising machines. Using this formulation to explore and compare the operational mechanisms of BLIM and OIM may lead to progress on a central question: how exactly do Ising machines work?

The remainder of the paper is organized as follows. In Sect. 2, we provide background on Ising models, oscillator Ising machines and latches. In Sect. 3, we set up a suitable system of equations for coupled latches, abstract them to a generalized form, and prove our main result: that the system has a Lyapunov function that matches a corresponding Ising Hamiltonian for high values of latch gain. Illustrative examples are provided in Sect. 4.

## 2 Background

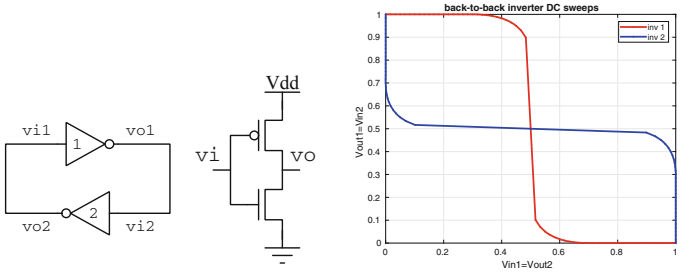


(a) Schematic.

(b) Butterfly curves (Shichman-Hodges MOSFET device model).

**Fig. 1.** Back to back inverters implement a bistable latch.

### 2.1 The Ising Model

The Ising model is simply a weighted graph, *i.e.*, a collection of nodes/vertices and branches/edges between some pairs of nodes, with each branch having a real-number weight. Each node (termed a "spin" in this context) is allowed to

[1] BLIM is not limited to electronic latches; it can use latches from any domain, *e.g.*, biochemical latches [5,6].

[2] This "energy" is not obviously related to any concept of physical energy, which latches, like all practical electronic elements, consume and dissipate as heat.

take two values, either 1 or −1. Associated with this graph is an expression, the **Ising Hamiltonian**, which multiplies the weight of each branch by the values of the two spins it connects to, and sums over all branches, *i.e.*,

$$H = -\frac{1}{2}\sum_{i,j=1}^{N} J_{ij}\, s_i s_j, \qquad \text{where } J_{ij} = J_{ji},\ \ J_{ii} = 0,\ \text{and } s_i \in \{-1,\ \ +1\} \quad (1)$$

are the $N$ spins. $J_{ij}$ are the branch weights, also called coupling coefficients. Owing to the Ising problem's origins for modelling and explaining ferromagnetism [4], Ising Hamiltonians are sometimes interpreted as an "energy" associated with a given configuration of the spins, although in recent computational applications they usually have no connection with energy in physics. The "Ising problem" is to find spin configurations with the minimum possible energy.

## 2.2 Latches

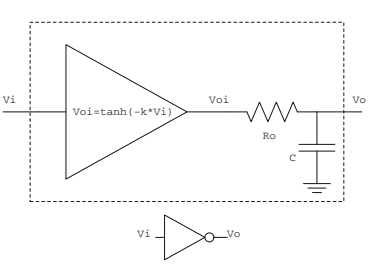


(a) tanh + output resistance/capacitance inverter model.

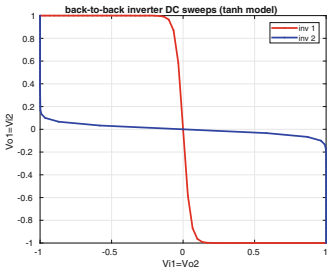


(b) Latch butterfly curves (tanh inverter model).

**Fig. 2.** tanh() + output resistance/capacitance inverter model and corresponding latch butterfly curves.

A fundamental element in electronics, the latch is perhaps most easily understood as two back-to-back inverters, as shown in Fig. 1(a), with each inverter consisting of the 2-transistor circuit shown at the right. Latches are ubiquitous in digital systems, in which they are the basis for, *e.g.*, registers and SRAM (static random access memory); as such, they are among the most compact and power-efficient elements in CMOS electronics.[3] That they are bistable becomes apparent when the I/O curves of both inverters are depicted on the same axes to produce so-called butterfly curves, shown in Fig. 1(b) (generated using the Shichman-Hodges model [13] for the MOSFETs).

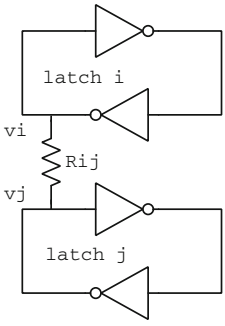


**Fig. 3.** Coupling between latches $i$ and $j$.

[3] When not switching, CMOS consumes no power beyond leakage losses.

The three intersections are the DC solutions (*i.e.*, equilibria) of the circuit. The intersection in the middle can be shown to be dynamically unstable,[4] leaving two stable solutions. The nature of the curves in Fig. 1(b), and the intersections that lead to bistability, are the essential feature of any latch, be it electronic or from any other domain (*e.g.*, biological [5,6]).

For concreteness and ease of exposition, we abstract each inverter using a $\tanh(\cdot)$ voltage transfer characteristic[5] followed by an output resistance and load capacitor, as shown in Fig. 2(a). The voltage I/O characteristic is $v_{oi} = \tanh(-kv_i)$, where the parameter $k > 0$ controls the gain, or sharpness, of the inverter characteristic. No current is drawn at the input; in the absence of loading at the output, the output voltage $v_o = v_{oi}$ (at DC). The corresponding butterfly curves, for $k = 20$, are shown in Fig. 2(b)—note their similarity to the ones in Fig. 1(b) for CMOS inverters.

The capacitor in Fig. 2(a) introduces dynamics, resulting in the following differential equation for a single inverter in the absence of additional load at $v_o$:

$$C\frac{dv_o(t)}{dt} = \frac{\tanh(-kv_i(t)) - v_o(t)}{R_o} = -\frac{\tanh(kv_i(t)) + v_o(t)}{R_o}. \tag{2}$$

To model a latch, *i.e.*, two back-to-back inverters are connected as in Fig. 1(a). (2) is repeated for the output of each inverter, resulting in

$$C\frac{dv_{i1}(t)}{dt} = -\frac{\tanh(kv_{i2}(t)) + v_{i1}(t)}{R_o},\ C\frac{dv_{i2}(t)}{dt} = -\frac{\tanh(kv_{i1}(t)) + v_{i2}(t)}{R_o}, \tag{3}$$

where the fact that the output of each inverter is the input of the other has been used. If we simplify the latch's dynamical representation by ignoring one of the inverter capacitors (*e.g.*, the one at the output of the first inverter $v_{o1} = v_{i2}$; this does not sacrifice any essential aspect of the latch's operation), (3) simplifies to the single differential equation

$$C\frac{dv(t)}{dt} = -\frac{\tanh\big(-k\tanh(kv(t))\big) + v(t)}{R_o} = \frac{\tanh\big(k\tanh(kv(t))\big) - v(t)}{R_o}, \tag{4}$$

where $v(t) \triangleq v_{i1}(t)$. (4) is the starting point for establishing the key result in Sect. 3, *i.e.*, that interconnected systems of latches can function as Ising machines.

## 3 Latch Ising Machines: A General Lyapunov Formulation

We now set up a network of coupled latches. Each coupling is realized using a resistor, as shown in Fig. 3. The coupling from the $j^{\text{th}}$ latch appears as an extra term in (4) for the $i^{\text{th}}$ latch, whose equation becomes

[4] *i.e.*, any small perturbation (*e.g.*, due to noise) from this solution will make the latch settle to one of the other two solutions, at the top left and bottom right.

[5] tanh() is merely a convenient analytical choice; any other smoothed step-like function can be used instead.

$$C\frac{dv_i(t)}{dt} = \frac{\tanh\left(k\tanh(kv_i(t))\right) - v_i(t)}{R_o} - \frac{v_i - v_j}{R_{ij}} \\ = G\tanh\left(k\tanh(kv_i(t))\right) - Gv_i(t) - J_{ij}(v_i - v_j), \tag{5}$$

where $G \triangleq \frac{1}{R_o}$ and $J_{ij} \triangleq \frac{1}{R_{ij}}$. For $N$ latches, this becomes a system of $N$ differential equations:

$$\frac{dv_i(t)}{dt} = \frac{1}{C}\left[G\tanh\left(k\tanh(kv_i(t))\right) - Gv_i(t) - \sum_{j=1}^{N} J_{ij}(v_i - v_j)\right], \\ i = 1, \cdots, N. \tag{6}$$

(6) can be written in a more general form, as

$$\frac{dv_i(t)}{dt} = f(v_i; k) - \sum_{j=1}^{N} J_{ij}\, g(v_i, v_j; k), \quad i = 1, \cdots, N; \tag{7}$$

choosing

$$f(v_i; k) = \frac{G}{C}\left(\tanh\left(k\tanh(kv_i)\right) - v_i\right) \text{ and } g(v_i, v_j; k) = \frac{v_i - v_j}{C} \tag{8}$$

turns it into (6). The utility of (7) over (6) is its generality: coupled networks of any kind of latch can be represented by appropriate choice of $f(\cdot;\cdot)$ and $g(\cdot,\cdot;\cdot)$. Indeed, (7) is not limited to latch networks; *e.g.*, OIM using the the Kuromoto model with SHIL [15], for coupled oscillator systems, is also captured, by setting

$$f(\Delta\phi_i; A_s) = \frac{A_s}{\omega_0}\sin\left(2\Delta\phi_i\right) \text{ and } g(\Delta\phi_i, \Delta\phi_j; A_s) = -\frac{A_c}{\omega_0}\sin\left(\Delta\phi_i - \Delta\phi_j\right). \tag{9}$$

The development in the remainder of this section does not use the specific form of the $\tanh(\cdot)$ latch model (6); instead, it uses the more general form of (7), thereby being applicable to different latch models, as well as OIM and potentially other manifestations of Ising machines. We prove two key results: 1) that there is a Lyapunov function (11) for (7),[6] and 2) that for high values of $k$, at which latches exhibit bistability, the Lyapunov function matches the Ising Hamiltonian (Theorem 2). In other words, the same underlying properties that enable coupled oscillator systems to serve as Ising machines hold for coupled latch systems.

### 3.1 Lyapunov Function

As already noted, the coupling is assumed to be symmetric, with no "self coupling",[7] *i.e.*,

[6] The Lyapunov function is defined in terms of abstract functions $z(\cdot;\cdot)$ and $h(\cdot,\cdot;\cdot)$ that are related to the functions $f(\cdot;\cdot)$ and $g(\cdot,\cdot;\cdot)$ in the generalized model (7). The relations, captured abstractly as assumptions in Assumption 2, are illustrated concretely for the $\tanh(\cdot)$ latch model in Sect. 4.

[7] This assumption is intrinsic to the Ising model, as already noted in (1).

**Assumption 1** (Coupling properties)

$$J_{ij} = J_{ji}, \quad J_{ii} = 0, \quad i, j = 1, \cdots, N. \tag{10}$$

We now define a scalar function of the $\{v_i\}$ that we will show satisfies the properties of a Lyapunov function. The functions $z(\cdot;\cdot)$ and $h(\cdot,\cdot;\cdot)$ used in the definition are left abstract at this point; specific choices for BLIM will be made in (39) and (41), later.

**Definition 1 (Lyapunov function $L(\cdots)$).** *Define*

$$L(v_1, \cdots, v_N;\, k) \triangleq -\sum_{i=1}^{N} \left( z(v_i;\, k) - \sum_{j=1}^{N} J_{ij}\, h(v_i, v_j;\, k) \right). \tag{11}$$

*Denoting $\vec{v} \triangleq [v_1, \cdots, v_N]^T$, we will also write this as $L(\vec{v};\, k)$. $z(v;\, k)$ and $h(v_1, v_2; k)$ are continuous and differentiable functions with properties to be stated later. Hence $L(\vec{v};\, k)$ is continuous and differentiable.*

We now assume that $z(\cdot;\,\cdot)$ and $h(\cdot,\cdot;\,\cdot)$ in (11) satisfy the following properties and relations to $f(\cdot;\,\cdot)$ and $g(\cdot,\cdot;\,\cdot)$. The first assumption (12) is essentially a definition of $z(\cdot;\,\cdot)$, used in the Lyapunov function, in terms of the abstraction $f(\cdot;\,\cdot)$ of the $\tanh(\cdot)$ latch model, used in (7). The second assumption captures the essential relation between the abstracted coupling function $g(\cdot,\cdot;\,\cdot)$ in (7), and the corresponding function $h(\cdot,\cdot;\,\cdot)$ in the Lyapunov expression in (11). This relation is required in order to show (in Theorem 1, below) that (11) is indeed a Lyapunov function for (7).

**Assumption 2** (**Properties of $z(\cdot;\,\cdot)$ and $h(\cdot,\cdot;\,\cdot)$**)

*1. $f(\cdot)$ in (8) is the derivative of $z(\cdot)$ in (11):*

$$f(v_m;\, k) = \frac{dz(v_m;\, k)}{dv_m}, \quad m = 1, \cdots, N. \tag{12}$$

*2. $h(\cdot,\cdot)$ in (11) and $g(\cdot,\cdot)$ in (8) are related as:*

$$g(v_m, v_j;\, k) = \frac{\partial h(v_m, v_j;\, k)}{\partial v_m} + \frac{\partial h(v_j, v_m;\, k)}{\partial v_m}. \tag{13}$$

**Theorem 1** ((11) **is a Lyapunov Function).** *If (12) and (13) hold and if the coupling is symmetric (10), then the function $L(\cdots)$ defined in (11) is a Lyapunov function for the system (7).*

*Proof. First, note that*

$$\frac{dL}{dt} = \sum_{m=1}^{N} \frac{\partial L}{\partial v_m} \frac{dv_m}{dt}. \tag{14}$$

*Expand*

$$\begin{aligned}
\frac{\partial L}{\partial v_m} &= -\left[\frac{dz(v_m;\,k)}{dv_m} - \frac{\partial}{\partial v_m}\left(\sum_{i,j=1}^{N} J_{ij}\, h(v_i, v_j;\,k)\right)\right] \\
&= -\left[\frac{dz(v_m;\,k)}{dv_m} - \sum_{i,j=1}^{N} J_{ij}\left(\frac{\partial h(v_i, v_j;\,k)}{\partial v_i}\delta_{im} + \frac{\partial h(v_i, v_j;\,k)}{\partial v_j}\delta_{jm}\right)\right] \\
&= -\left[\frac{dz(v_m;\,k)}{dv_m} - \sum_{i,j=1}^{N} J_{ij}\frac{\partial h(v_i, v_j;\,k)}{\partial v_i}\delta_{im} - \sum_{i,j=1}^{N} J_{ij}\frac{\partial h(v_i, v_j;\,k)}{\partial v_j}\delta_{jm}\right] \\
&= -\left[\frac{dz(v_m;\,k)}{dv_m} - \sum_{j=1}^{N} J_{mj}\frac{\partial h(v_m, v_j;\,k)}{\partial v_m} - \sum_{i=1}^{N} J_{im}\frac{\partial h(v_i, v_m;\,k)}{\partial v_m})\right] \\
&= -\left[\frac{dz(v_m;\,k)}{dv_m} - \sum_{j=1}^{N} J_{mj}\frac{\partial h(v_m, v_j;\,k)}{\partial v_m} - \sum_{j=1}^{N} J_{jm}\frac{\partial h(v_j, v_m;\,k)}{\partial v_m}\right] \\
&= -\left[\frac{dz(v_m;\,k)}{dv_m} - \sum_{j=1}^{N} J_{mj}\frac{\partial h(v_m, v_j;\,k)}{\partial v_m} - \sum_{j=1}^{N} J_{mj}\frac{\partial h(v_j, v_m;\,k)}{\partial v_m}\right] \quad \textit{(using (10))} \\
&= -\left[\frac{dz(v_m;\,k)}{dv_m} - \sum_{j=1}^{N} J_{mj}\left(\frac{\partial h(v_m, v_j;\,k)}{\partial v_m} + \frac{\partial h(v_j, v_m;\,k)}{\partial v_m}\right)\right] \qquad (15) \\
&= -\left[f(v_m;\,k) - \sum_{j=1}^{N} J_{mj}\, g(v_m, v_j;\,k)\right] \quad \textit{(using (12) and (13))} \\
&= -\frac{dv_m}{dt} \quad \textit{(using (7))}. \qquad (16)
\end{aligned}$$

*Using* (16), (14) *becomes*

$$\frac{dL}{dt} = -\sum_{m=1}^{N}\left(\frac{dv_m}{dt}\right)^2 \leq 0, \qquad (17)$$

*proving that* $L(\cdots)$ *is non-increasing in* $t$*, hence constitutes a Lyapunov function for* (7). ■

**Lemma 1 (Stable equilibria and Lyapunov local minima are identical).** *Any stable equilibrium of the generalized system* (7) *is a local minimum of the generalized Lyapunov function* (11)*; and vice versa.*

*Proof. Using* (16)*, we can write* (7) *as*

$$\frac{dv_i}{dt} = -\frac{\partial L}{\partial v_i}, \quad i = 1, \cdots, N. \qquad (18)$$

*Given any equilibrium point* $\vec{v}^* \triangleq [v_1^*, \cdots, v_N^*]^T$*, i.e.,* $\frac{dv_i}{dt} = 0,\ \forall i$*. By* (18)*, the partial derivatives* $\frac{\partial L(\vec{v}^*)}{\partial v_i} = 0, \forall i$*, i.e., the equilibrium point is a local extremum (maximum/minimum/saddle/etc.. point) of* $L(\cdots)$.

*Suppose $\vec{v}^*$ is a **stable** equilibrium. This means that there exists some ball $\mathcal{B}$ around $\vec{v}^*$, with radius greater than zero, such that if the system is perturbed to any point $\vec{v}^* + \delta\vec{v} \in \mathcal{B}$, the system's dynamics will return it to $\vec{v}^*$. More precisely, the projection of the derivative $\frac{d(\vec{v}^* + \delta\vec{v}(t))}{dt}$ onto the perturbation $\delta\vec{v}$ should be negative, i.e.,*

$$\delta\vec{v}^T \frac{d}{dt}(\vec{v}^* + \delta\vec{v}) < 0, \quad \forall\, \delta\vec{v} \;\; \textit{such that } \vec{v}^* + \delta\vec{v} \in \mathcal{B}. \tag{19}$$

*Using (18), (19) becomes*

$$\underbrace{\left.\frac{\partial L}{\partial \vec{v}}\right|_{\vec{v}^*+\delta\vec{v}}}_{\textit{Jacobian of } L \textit{ w.r.t } \vec{v} \textit{ (row vector)}} \delta\vec{v} > 0, \quad \forall\, \delta\vec{v} \;\; \textit{such that } \vec{v}^* + \delta\vec{v} \in \mathcal{B}. \tag{20}$$

*Since $L(\vec{v};\, k)$ is differentiable (Definition 1), we have*

$$L(\vec{v}^*) \simeq L(\vec{v}^* + \delta\vec{v}) - \left.\frac{\partial L}{\partial \vec{v}}\right|_{\vec{v}^*+\delta\vec{v}} \delta\vec{v} \Leftrightarrow L(\vec{v}^* + \delta\vec{v}) - L(\vec{v}^*) \simeq \left.\frac{\partial L}{\partial \vec{v}}\right|_{\vec{v}^*+\delta\vec{v}} \delta\vec{v}, \tag{21}$$

*with equality as $\delta\vec{v} \to \vec{0}$. Using (20) in (21), we have $L(\vec{v}^* + \delta\vec{v}) - L(\vec{v}^*) > 0$ for all $\delta\vec{v}$ such that $\vec{v}^* + \delta\vec{v}$ is in some ball $\mathcal{B}_2 \subset \mathcal{B}$, proving that $v^*$ is a local **minimum** of $L(\vec{v};\, k)$.*

*Moreover, every step of the above argument can be reversed, proving that any local minimum of $L(\vec{v};\, k)$ is a stable equilibrium point of (7).* ■

### 3.2 Bistability Properties of the Generalized System; Lyapunov–Ising-Hamiltonian Relation

First, we recall the (discrete) Ising Hamiltonian and establish a basic property.

**Definition 2 (Discrete Ising Hamiltonian).** *Given $N$ "spins" (binary variables with values $\pm 1$) $\{s_i\}$ and a set of coupling weights $J_{ij}$ obeying (10), the (discrete) Ising Hamiltonian of the system is*

$$H(s_1, \cdots, s_N) \triangleq -\frac{1}{2} \sum_{i,j=1}^{N} J_{ij}\, s_i s_j. \tag{22}$$

*Denoting $\vec{s} = [s_1, \cdots, s_N]^T$, this can also be written as $H(\vec{s})$.*

**Lemma 2 (Scaled/shifted Ising Hamiltonians preserve total order).** *For any $k_1 > 0$ and any $k_2$, define a scaled/shifted version of the Ising Hamiltonian to be*

$$\tilde{H}(\vec{s}) \triangleq k_1 H(\vec{s}) + k_2. \tag{23}$$

*Then, for any $\vec{s}_1$, $\vec{s}_2$ such that $H(\vec{s}_1) \leq H(\vec{s}_2)$, $\tilde{H}(\vec{s}_1) \leq \tilde{H}(\vec{s}_2)$; and vice-versa. This also implies that any local minimum of $H(\cdot)$ is a local minimum of $\tilde{H}(\cdot)$, and vice versa.*

*Proof.* $\tilde{H}(\cdot)$ *is strictly monotonic and invertible with respect to* $H(\cdot)$*, establishing both directions of the first claim. The second claim follows from the first by contradiction.*

Next, we make an assumption about the bistability of $f(\cdot;k)$ when the gain $k$ is high.

**Assumption 3 (Bistability of each latch).** $f(v;\,k)$ *is bistable if* $k=K$*, for some sufficiently large gain* $K>0$*; i.e., for some* $v_+, v_-$*, with* $v_+ > v_-$*,*

$$f(v_+;K) = f(v_-;K) = 0. \tag{24}$$

*Moreover,*

$$\left.\frac{df(v;K)}{dv}\right|_{v=v_+} < 0 \quad \textit{and} \quad \left.\frac{df(v;K)}{dv}\right|_{v=v_-} < 0. \tag{25}$$

*These conditions ensure stable equilibria of* $\frac{dv}{dt} = f(v;\,K)$ *(i.e., each equation of the generalized system (7), in the absence of coupling) at* $v_+$ *and* $v_-$*. Moreover, we assume that for each latch,* $v_+$ *and* $v_-$ *are the only stable equilibria. This implies that* $v_i \in \{v_+, v_-\}$*,* $i=1,...,N$ *represent all the stable equilibria of (7) in the absence of coupling.*

We now make assumptions on the values of the functions $z(\cdot;\ \cdot)$ and $h(\cdot,\cdot;\,\cdot)$ at the bistable values $v_+$ and $v_-$ when the gain is high. These assumptions are abstracted from properties of the $\tanh(\cdot)$ model (8).

**Assumption 4 (Values for** $z(\{v_+,v_-\};\ K)$ **and** $h(\{v_+,v_-\},\{v_+,v_-\};\,K)$**)**

$$z(v_+;\,K) = z(v_-;\,K) = c_3 \tag{26}$$

$$h(v_+,v_+;\,K) = h(v_-,v_-;\,K) = c_1, \tag{27}$$

$$h(v_+,v_-;\,K) = h(v_-,v_+;\,K) = c_2. \tag{28}$$

*for some values* $c_1$*,* $c_2 > c_1$ *and* $c_3$*.*

We can now establish a relation between the generalized Lyapunov function $L(\cdots)$ in (7) and the Ising Hamiltonian (22).

**Theorem 2 (The Lyapunov function equals a scaled/shifted Ising Hamiltonian at nominal bistable values).** *For* $i=1,\cdots,N$*, if* $v_i \in \{v_+,v_-\}$*, define a corresponding "spin"* $s_i$ *to be*

$$s_i = \begin{cases} 1 & \textit{if } v_i = v_+, \\ -1 & \textit{if } v_i = v_-. \end{cases} \tag{29}$$

*Denote* $\vec{s} \triangleq [s_1,\cdots,s_N]^T$ *and* $\vec{v}_B \triangleq [v_1,\cdots,v_N]^T$*. Then the generalized Lyapunov function* $L(\vec{v}_B;\,K)$ *equals a scaled/shifted version of the discrete Ising Hamiltonian* $H(\vec{s})$*.*

*Proof. We have (using (26))*

$$\begin{aligned} L(\vec{v}_B;\, K) &= -\sum_{i=1}^{N}\left(z(v_i;\, K) - \sum_{j=1}^{N} J_{ij}\, h(v_i, v_j;\, K)\right) \\ &= -Nc_3 + \sum_{i,j=1}^{N} J_{ij}\, h(v_i, v_j;\, K). \end{aligned} \tag{30}$$

*Defining*

$$\begin{aligned} \tilde{h}(v_i, v_j) &\triangleq \frac{2h(v_i, v_j;\, K) - (c_1 + c_2)}{c_2 - c_1} \\ \Leftrightarrow h(v_i, v_j;\, K) &= \frac{(c_2 - c_1)\tilde{h}(v_i, v_j) + (c_1 + c_2)}{2}, \end{aligned} \tag{31}$$

(30) *becomes*

$$\begin{aligned} L(\vec{v}_B;\, K) &= -Nc_3 + \frac{1}{2}\sum_{i,j=1}^{N} J_{ij}\left[(c_2 - c_1)\,\tilde{h}(v_i, v_j) + (c_1 + c_2)\right] \\ &= -Nc_3 + \frac{c_1 + c_2}{2}\left(\sum_{i,j=1}^{N} J_{ij}\right) + \frac{c_2 - c_1}{2}\sum_{i,j=1}^{N} J_{ij}\,\tilde{h}(v_i, v_j). \end{aligned} \tag{32}$$

*From definition (31), note that*

$$\tilde{h}(v_+, v_+) = \tilde{h}(v_-, v_-) = -1, \quad \tilde{h}(v_+, v_-) = \tilde{h}(v_-, v_+) = +1. \tag{33}$$

*Hence, since $v_i \in [v_+, v_-]$, we have*

$$\tilde{h}(v_i, v_j) = -s_i s_j. \tag{34}$$

*Using (34) in (32), we have*

$$\begin{aligned} L(\vec{v}_B;\, K) &= -Nc_3 + \frac{c_1 + c_2}{2}\left(\sum_{i,j=1}^{N} J_{ij}\right) - \frac{c_2 - c_1}{2}\sum_{i,j=1}^{N} J_{ij}\, s_i s_j \\ &= \underbrace{-Nc_3 + \frac{c_1 + c_2}{2}\left(\sum_{i,j=1}^{N} J_{ij}\right)}_{k_2} + \underbrace{(c_2 - c_1)}_{k_1 > 0} H(\vec{s}). \end{aligned} \tag{35}$$

*This is a scaled/shifted version of the Ising Hamiltonian (23).* ■

This immediately implies

**Corollary 1 (Total order correspondence between Hamiltonian and Lyapunov functions).** *For $i = 1, \cdots, N$, let*

$$\begin{aligned} \vec{v}_A \triangleq [v_{A,1}, \cdots, v_{A,N}]^T, \quad \vec{v}_B \triangleq [v_{B,1}, \cdots, v_{B,N}]^T, \\ \text{with } v_{A,i} \in \{v_+, v_-\},\ v_{B,i} \in \{v_+, v_-\}. \end{aligned} \tag{36}$$

*Let $\vec{s}_A$ and $\vec{s}_B$ be the spin vectors (defined using (29)) corresponding to $\vec{v}_A$ and $\vec{v}_B$, respectively. If $L(\vec{v}_A; K) \leq L(\vec{v}_B; K)$, then $H(\vec{s}_A) \leq H(\vec{s}_B)$; and vice versa.*

*Proof. Follows from Lemma 2 and Theorem 2.*

As a result, any global minimum of one is also one of the other:

**Corollary 2 (Hamiltonian and Lyapunov global minima correspond under bistability).** *If $\vec{v}_A$ (36) is a global minimum of $L(\vec{v}; K)$ over all $\vec{v}$ with components taking bistable values $v_+$ or $v_-$, then the corresponding spin vector $s_A$ (29) is a global minimum of $H(\vec{s})$; and vice versa.*

*Proof. Follows from Corollary 1.*

Even with coupling present in (7), we assume that each latch remains bistable, with only small deviations from $v_+$ and $v_-$:

**Assumption 5 (Bistability persists in the presence of coupling).** *In the presence of coupling, the exact values $v_+$ and $v_-$ (Assumption 3) no longer represent stable equilibria for each latch, due to the perturbations introduced by the coupling. If the coupling is small enough, each latch will still have stable equilibria at some values $v_{i+}$ and $v_{i-}$ which are small perturbations of $v_+$ and $v_-$, respectively. This follows from the stability of the unperturbed equilibria. We assume, more generally, that this is true whether or not the coupling is small. More precisely, we assume that if $k = K$, then $v_i \in \{v_{i+}, v_{i-}\}$, with $v_{i+} \in [v_+ - \epsilon, v_+ + \epsilon]$ and $v_{i-} \in [v_- - \epsilon, v_- + \epsilon]$, for some $\epsilon \ll v_+ - v_-$, $\forall i = 1, \cdots, N$ capture **all stable equilibrium points** of (7).*

Assumption 5 enables us to benefit from Theorem 2 at the actual equilibrium points of (7):

**Corollary 3 (Lyapunov function approximates a scaled/shifted Ising Hamiltonian at bistable values).** *The Lyapunov function evaluated at bistable equilibrium points in the presence of coupling (as given in Assumption 5) approximates the scaled/shifted Ising Hamiltonian (35) at corresponding spin values.*

*Proof. Follows from continuity of the Lyapunov function (11) in its arguments $v_1, \cdots, v_N$, and the fact that the bistable equilibrium points under coupling are small perturbations (Assumption 5) of the nominal bistable equilibria of Theorem 2.*

Finally, note that the discrete Ising Hamiltonian (Definition 2) remains unchanged when all spins are flipped, since each term $s_i s_j$ does not change. Correspondingly, the Lyapunov function (11) remains unchanged if $v_i$ is "flipped" from $v_+$ to $v_-$, and vice-versa (because of properties (26) to (28)). This implies that the search space of all Boolean combinations can be reduced by half; one spin can simply be set to either $+1$ or $-1$, and all combinations of the other spins explored. Correspondingly, for *one* chosen $i \in \{1, \cdots, N\}$, $v_i$ can be set to either $v_+$ or $v_-$. We concretize this as

**Corollary 4.** *Let $k = K$ and $v_i \in \{v_+, v_-\}$ for $i \in 1, \cdots, N$. Then $v_N$ can be fixed at $v_+$ without loss of generality, i.e., every value of the Lyapunov function (11) $L(v_1, \cdots, v_N;\, K)$ that can be achieved without this restriction can also be achieved with this restriction.*

## 4 Illustrative Examples

We now specialize the above results for our simple latch model of Sect. 2.2 and illustrate BLIM on fully-connected 3-spin graphs, as well as on G22, a 2000-spin, sparsely connected, MAX-CUT benchmark.

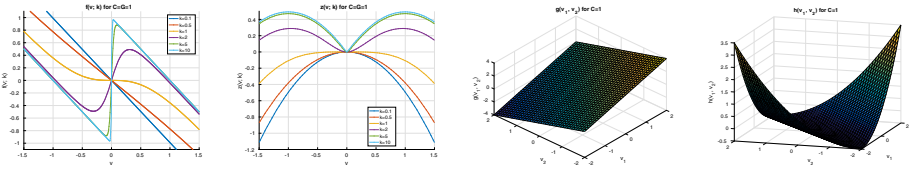

(a) $f(v;\, k)$ (b) $z(v;\, k)$ (c) $g(v_1, v_2;\, k)$ (d) $h(v_1, v_2;\, k)$

**Fig. 4.** Plots of $f()$, $g()$, $z()$ and $h()$ for $C = G = 1$.

First, we return to our $\tanh(\cdot)$ latch model of (6) and devise a specific Lyapunov function ((11)) for it. Recall that $f(\cdot;\, k)$ and $g(\cdot, \cdot;\, k)$ for this model are given in (8). Choosing the high value of gain (at which each latch features two stable states, see Assumption 3) to be

$$K \triangleq 5, \tag{37}$$

we solve $f(v;\, K) = 0$ numerically to obtain[8]

$$\begin{aligned} &v_+ \triangleq 0.999909 \simeq +1, \quad v_- \triangleq -0.999909 = -v_+ \simeq -1, \\ &\frac{df}{dv}(v_+) = -0.999999 < 0, \quad \frac{df}{dv}(v_-) = -0.999999 < 0. \end{aligned} \tag{38}$$

Hence Assumption 3 is satisfied.[9] Assumption 5 can always be satisfied by making the couplings small enough. Define

$$z(v;\, k) \triangleq \int_0^v f(x;\, k)\, dx. \tag{39}$$

This obviously satisfies the requirement (12). Since $f(v;\, k)$ is odd in $v$ (*i.e.*, $f(-v;\, k) = -f(v;\, k)$, as is easily verified), it is easily shown that $z(v;\, k)$ in (39) is even, *i.e.*,

$$z(-v;\, k) = z(v;\, k). \tag{40}$$

[8] It is easy to show graphically that $v_+$, $v_-$ and 0 are the only solutions of $f(v, K) = 0$.
[9] The third solution, $v = 0$, is unstable: $\frac{df}{dv}(0) = 24 > 0$.

Hence the requirement (26) is satisfied. Now define

$$h(v_i, v_j;\, k) \triangleq \frac{1}{2C}\left[\frac{(v_i - v_j)^2}{2} - 1\right]. \tag{41}$$

It is easily verified that $h(v_i, v_j;\, k)$ satisfies the requirement (13). The additional requirements (27) and (28) are also satisfied, with

$$c_1 = -\frac{1}{2C}, \quad c_2 = \frac{1}{2C}(2v_+^2 - 1) \simeq -c_1 = \frac{1}{2C} > c_1. \tag{42}$$

Hence, using the definitions in (37) to (39) and (41) for $K$, $v_+$, $v_-$, $z(v;\, k)$ and $h(v_i, v_j;\, k)$, the coupled latch system (6) satisfies all the conditions needed for Theorem 1, Theorem 2, and their implications Lemma 1, Corollary 1, Corollary 2 and Corollary 3 to be valid. To summarize:

1. the behaviour of a system of coupled latches (6), for any latch gain $k$, is governed by a Lyapunov function which it minimizes locally to reach stable equilibria;
2. when the gain is high enough to make each latch bistable ($k = K$), a scaled/shifted version of the Lyapunov function closely approximates the system's discrete Ising Hamiltonian (Definition 2). This implies that if $H(\vec{s}_A) \leq H(\vec{s}_B)$ for any two spin states, the corresponding voltage states $\vec{v}_A$ and $v_B$ obey $L(\vec{v}_A;\, K) \leq L(\vec{v}_A;\, K)$; and vice versa.[10] Moreover, global minima of the Ising Hamiltonian correspond to global minima of the Lyapunov function.

Plots of $f(v;\, k)$, $g(v_1, v_2;\, k)$, $z(v;\, k)$ and $h(v_1, v_2;\, k)$—equations (8), (39) evaluated numerically, and (41)—are shown in Fig. 4, for different values of the latch gain $k$.

### 4.1 Fully-Connected 3-Spin Graphs with Weights of Equal Magnitude

For insight, we explore BLIM on all fully-connected 3-spin graphs with weights of equal magnitude. We choose 3-spin graphs because their Lyapunov functions can be visualized completely in three dimensions.

A three-spin graph is a triangle, *i.e.*, with three vertices and three edges with weights $J_{12}$, $J_{23}$ and $J_{13}$. The Ising Hamiltonian (Definition 2) is

$$H_3(s_1, s_2, s_3) \triangleq -\frac{1}{2}\left(J_{12}\, s_1 s_2 + J_{13}\, s_2 s_3 + J_{23} s_1 s_3\right), \tag{43}$$

and the Lyapunov function becomes

$$\begin{aligned} L_3(v_1, v_2, v_3;\, k) \triangleq -z(v_1;\, k) - z(v_2; k) - z(v_3;\, k) + 2\big[J_{12}\, h(v_1, v_2;\, k) \\ + J_{23}\, h(v_2, v_3;\, k) + J_{13}\, h(v_1, v_3;\, k)\big], \end{aligned} \tag{44}$$

[10] Recall that $H(\cdot)$ is the Ising Hamiltonian and $L(\vec{\cdot}\,;\cdot)$ the Lyapunov function.

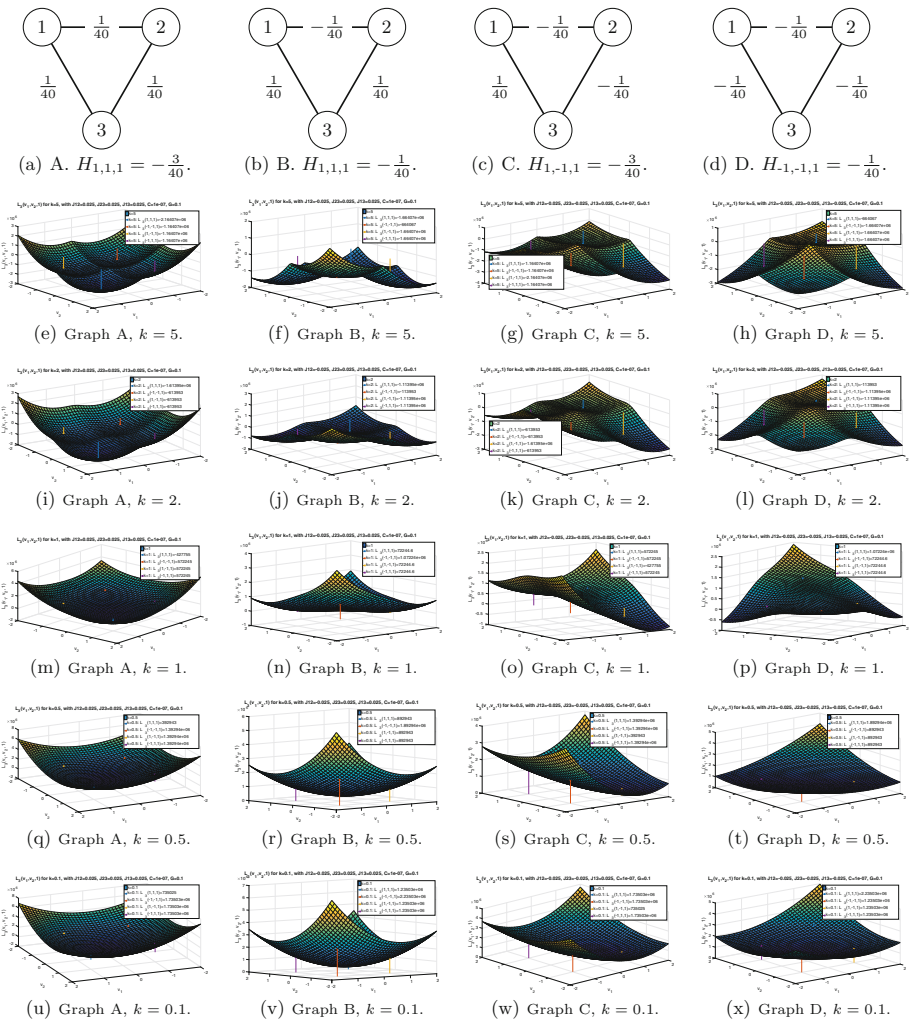


**Fig. 5.** $L_3(v_1, v_2, 1)$ for fully-connected 3-node graphs.

where $f(\cdot;\, k)$ and $h(\cdot, \cdot;\, k)$ are given by (39) and (41), and we have used the even symmetry of $h(\cdot, \cdot;\, k)$. Also, applying Corollary 4, we set $v_3 = v_+$, which turns (44) into

$$L_3(v_1, v_2, v_+;\, k) \triangleq -z(v_1;\, k) - z(v_2;\, k) - z(v_+;\, k) + 2\big[J_{12}\, h(v_1, v_2;\, k) + J_{23}\, h(v_2, v_+;\, k) + J_{13}\, h(v_1, v_+;\, k)\big], \tag{45}$$

Consider fully-connected graphs with edge weights $\pm A_c$, where $A_c$ is a coupling strength parameter. There are only 4 unique fully-connected 3-node graphs of

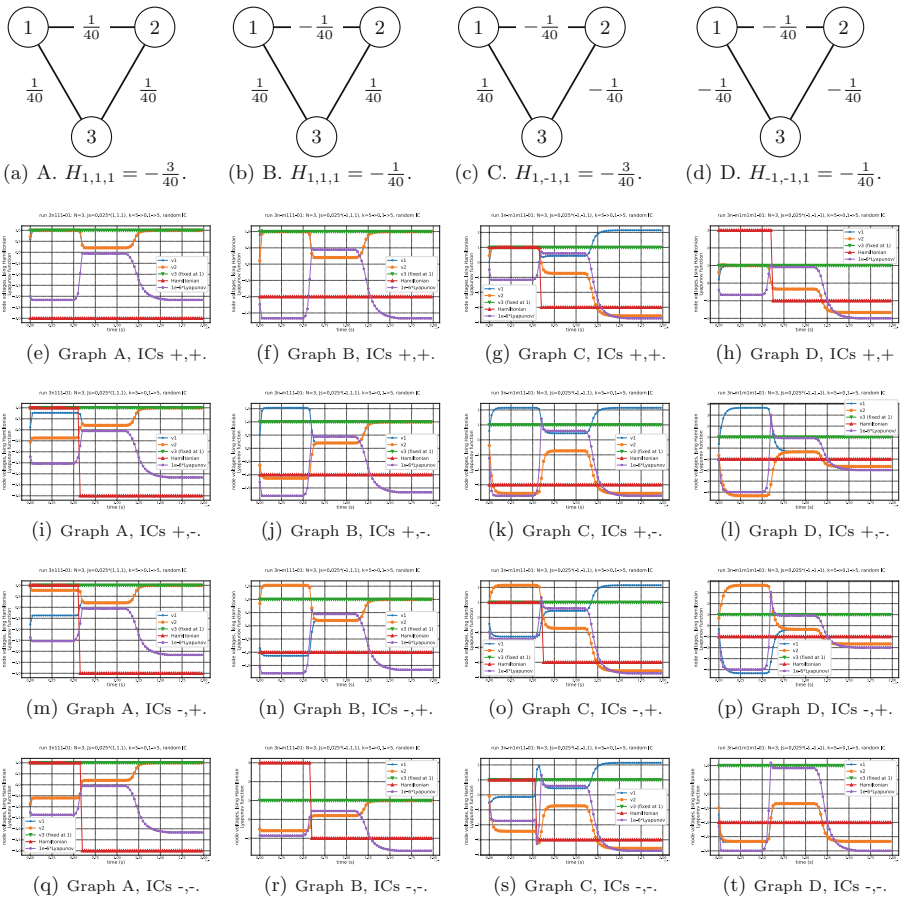


(a) A. $H_{1,1,1} = -\frac{3}{40}$. (b) B. $H_{1,1,1} = -\frac{1}{40}$. (c) C. $H_{1,\text{-}1,1} = -\frac{3}{40}$. (d) D. $H_{\text{-}1,\text{-}1,1} = -\frac{1}{40}$.

(e) Graph A, ICs +,+. (f) Graph B, ICs +,+. (g) Graph C, ICs +,+. (h) Graph D, ICs +,+

(i) Graph A, ICs +,-. (j) Graph B, ICs +,-. (k) Graph C, ICs +,-. (l) Graph D, ICs +,-.

(m) Graph A, ICs -,+. (n) Graph B, ICs -,+. (o) Graph C, ICs -,+. (p) Graph D, ICs -,+.

(q) Graph A, ICs -,-. (r) Graph B, ICs -,-. (s) Graph C, ICs -,-. (t) Graph D, ICs -,-.

**Fig. 6.** Simulations of (7) and (4) with different initial conditions for fully-connected 3-node graphs.

this type, as shown in the top row[11] of Fig. 5—other fully-connected graph possibilities are congruent to one of these. Figure 5 depicts the Lyapunov functions for all four fully-connected graphs—each column shows the Lyapunov functions for various values of $k$ for a particular graph. The points corresponding to discrete Ising spins, *i.e.*, $v_1, v_2 = \pm 1$, are marked with vertical lines and the Lyapunov values at these points are noted in the legend. As expected, high values of $k$ feature multiple local minima, which coalesce as $k$ is lowered below 1. For the case of weights $(-\frac{1}{40}, -\frac{1}{40}, -\frac{1}{40})$, where several points reach the global minimum, the Lyapunov landscape for low $k$ becomes more of a saddle region than a single well-defined global minimum.

[11] Each node represents an Ising spin; the weight of the edge between two nodes $i$ and $j$ is $J_{ij}$.

The Lyapunov result above (Theorem 1) only guarantees settling to *local* minima, for any fixed (unchanging with time) value of the gain $k$. However, we have observed empirically that changing $k$ from a high value to a low value and back again (over time) enables the system to break out of higher local minima and settle to lower ones. This is analogous to changing the amplitude of SYNC periodically in OIM and achieves the same end, *i.e.*, moving the system between discrete (binarized) and continuous (analog) modes of operation. In OIM, several such "ramps" of SYNC typically lead to excellent progress towards the global minimum, and we have observed a similar phenomenon with BLIM when $k$ is ramped several times. Indeed, examining how the Hamiltonian changes as ramping progresses reveals that improvements to the Hamiltonian occur predominantly when the system is *not* binarized, but is operating in continuous/analog mode, or is in transition between discrete and continuous modes.

Figure 6 shows results from simulating (7) and (8) for all fully-connected 3-node graphs, with $k$ changed from 5 to 0.1 and back to 5 over the simulation. $v_3$ is fixed at $+1$; initial conditions for $v_1$ and $v_2$ are chosen to be different combinations of positive and negative values (randomly generated) for each simulation. Note that in every case, $k$ ramping takes the system to a global minimum at $k = 5$. The reason for this is apparent upon examining the region $t \sim [60, 120]\mu$s, when $k = 0.1$ and the system has a unique global Lyapunov minimum to which it settles. Note that the values of $v_1$ and $v_2$ "lean towards" a $k = 5$ global minimum here, in every case. As a result, the system evolves quasi-statically to a $k = 5$ global minimum as $k$ is ramped back to 5.

### 4.2 G22 MAX-CUT Benchmark Problem

We also illustrate BLIM with several cycles of $k$-ramping on the G22 Ising benchmark problem [1,12]. The problem has $N = 2000$ nodes/spins, sparsely interconnected (with randomly generated $\pm 1$ weights) with 19,990 connections. Figure 7 shows the progress of the Ising Hamiltonian as BLIM runs on this problem, with $k$ ramped from 0.5 to 2 in a square wave fashion about 6 times over the simulation. As can be seen, subsequent cycles of $k$-ramping reduce the Hamiltonian; moreover, the reduction happens largely when $k$ is low, *i.e.*, the system is *not* binarized, but in analog mode. As with OIM and other Ising machine schemes, the underlying mechanism behind this is not well understood at this point but it is this feature, that some deep analog mechanism is solving the originally discrete Ising problem, that fundamentally separates Ising machines from hardware or software implementations of essentially discrete minimization methods [9,11].

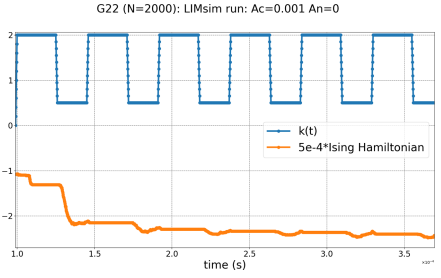


**Fig. 7.** BLIM on the 2000-spin Ising benchmark problem G22 [1,12]: the Hamiltonian improves when $k$ is low, *i.e.*, the system is in "analog mode".

## 5 Conclusion

We have presented BLIM, an Ising machine scheme based on latches (bistable elements) with controllable gains. Using a simple dynamical model that distills the essence of a back-to-back inverter-based latch, we have set up equations for coupled latch systems and shown that they can be generalized to a form that also captures coupled oscillator networks when two functions are defined appropriately. We have proved that under appropriate conditions, this generalized form has a Lyapunov function which becomes essentially identical to the Ising Hamiltonian when the system is driven to binarized states, *e.g.*, by making latch gains high. This result implies that the system will settle naturally to local minima of the Lyapunov function. Furthermore, varying the gains periodically is seen to lead the system to lower minima. Our general formulation enables side-by-side comparison of OIM, BLIM, and possibly other Ising machine schemes, which may lead to progress in unravelling the mechanisms that underlie Ising machines' intriguing global minimization tendencies. BLIM retains an important practical feature of OIM, *i.e.*, that it can be implemented using miniaturisable CMOS electronics; however, implementations in other physical domains, such as (synthetic) biology, may also be of interest.

**Acknowledgments.** We thank Tianshi Wang, Nagendra Krishnapura, Yiannis Tsividis and Peter Kinget for discussions that motivated this work. Support from the US National Science Foundation is gratefully acknowledged.

## References

1. The G-set benchmarks for MAX-CUT. http://grafo.etsii.urjc.es/optsicom/maxcut
2. Bian, Z., Chudak, F., Macready, W.G., Rose, G.: The Ising model: teaching an old problem new tricks. D-Wave Systems 2 (2010)
3. Wang, T., Roychowdhury, J.: OIM: oscillator-based Ising machines for solving combinatorial optimisation problems. In: McQuillan, I., Seki, S. (eds.) UCNC 2019. LNCS, vol. 11493, pp. 232–256. Springer, Cham (2019). https://doi.org/10.1007/978-3-030-19311-9_19 Preprint available at arXiv:1903.07163 [cs.ET] at arXiv:1903.07163 [cs.ET]
4. Brush, S.G.: History of the Lenz-Ising model. Rev. Mod. Phys. **39**(4), 883–893 (1967). https://doi.org/10.1103/RevModPhys.39.883
5. Comorosan, S.: New mechanism for the control of cellular reactions: the biochemical flip-flop. Nature **227**(5253), 64–65 (1970)
6. Endo, K., Hayashi, K., Inoue, T., Saito, H.: A versatile cis-acting inverter module for synthetic translational switches. Nature Commun. **4** (2013). https://doi.org/10.1038/ncomms3393
7. Gärtner, B., Matousek, J.: Approximation Algorithms and Semidefinite Programming. Springer, Heidelberg (2014). https://doi.org/10.1007/978-3-642-22015-9
8. Johnson, M.W., et al.: Quantum annealing with manufactured spins. Nature **473**(7346), 194–198 (2011)
9. Camsari, K.Y., Faria, R., Sutton, B.M., Datta, S.: Stochastic p-bits for invertible logic. Phys. Rev. X **7**(3), 031014 (2017)

10. Kirkpatrick, S., Gelatt, C.D., Vecchi, M.P.: Optimization by simulated annealing. Science **220**(4598), 671–680 (1983)
11. Yamaoka, M., Yoshimura, C., Hayashi, M., Okuyama, T., Aoki, H., Mizuno, H.: A 20k-spin Ising chip to solve combinatorial optimization problems with CMOS annealing. IEEE J. Solid-State Circ. **51**(1), 303–309 (2016)
12. Festa, P., Pardalos, P.M., Resende, M.G.C., Ribeiro, C.C.: Randomized heuristics for the MAX-CUT problem. Opt. Methods Softw. **17**(6), 1033–1058 (2002)
13. Shichman, H., Hodges, D.A.: Modeling and simulation of insulated-gate field-effect transistor switching circuits. IEEE J. Solid-State Ckts. **3**(3), 285–289 (1968)
14. Inagaki, T., et al.: A Coherent Ising machine for 2000-node optimization problems. Science **354**(6312), 603–606 (2016)
15. Wang, T., Roychowdhury, J.: Oscillator-based Ising machine. arXiv:1709.08102 (2017)
16. Wang, T., Wu, L., Roychowdhury, J.: New computational results and hardware prototypes for oscillator-based Ising machines. In: Proceedings of the IEEE DAC, pp. 239:1–239:2 (2019). https://doi.org/10.1145/3316781.3322473
17. Wang, T., Wu, L., Nobel, P., Roychowdhury, J.: Solving combinatorial optimisation problems using oscillator based Ising machines. Natural Comput., 1–20 (2021)
18. Haribara, Y., Utsunomiya, S., Yamamoto, Y.: Computational principle and performance evaluation of Coherent Ising Machine based on degenerate optical parametric oscillator network. Entropy **18**(4), 151 (2016)
19. Wang, Z., Marandi, A., Wen, K., Byer, R.L., Yamamoto, Y.: Coherent Ising machine based on degenerate optical parametric oscillators. Phys. Rev. A **88**(6), 063853 (2013)